Modeling of the Particle Size Distribution in Emulsion Polymerization

Ashwini Sood

Department of Chemical Engineering, Harcourt Butler Technological Institute, Kanpur 208 002, India

Received 5 May 2007; accepted 4 October 2007
DOI 10.1002/app.28083
Published online 17 April 2008 in Wiley InterScience (www.interscience.wiley.com).

ABSTRACT: A mathematical model to predict the evolution of the latex particle size distribution in an emulsion polymerization reactor was developed. The mathematical framework is based on the population balance approach. It is general in framework, readily expandable to incorporate the physiochemical phenomena of interest to the reacting system of interest. The model includes such mechanistic details as (1) particle generation from radicals entering micelles; (2) particle size dependence of the radical entry mechanism; (3) coupling of the radical concentration in the aqueous phase and the particle phase; (4) determination of the particle phase radical concentration by radical entry into, exit from, and termination inside the particle; and (5) thermodynamic equilibrium between the monomer concentration in the aqueous phase and the particle phase. The model was solved efficiently with orthogonal collocation. Dynamic simulations were compared with experimental data taken from the literature for the emulsion polymerization of styrene (monomer), potassium persulfate (initiator), and sodium dodecyl sulfate (emulsifier). The variables considered were the total number of particles formed, duration of the nucleation period, conversion at the end of the nucleation period, variation of the monomer volume fraction in the particles with time, and conversion–time curves for different monomer, initiator, and emulsifier concentrations. Close agreement was found between the simulations and the experimental data. © 2008 Wiley Periodicals, Inc. J Appl Polym Sci 109: 1403–1419, 2008

Key words: emulsion polymerization; growth; modeling; particle nucleation; particle size distribution

INTRODUCTION

Particle size distribution (PSD) is a key parameter in the emulsion polymerization process; it directly influences the final latex end-use properties, such as its rheological properties, maximum solid content, adhesion, drying time, film-forming characteristics, freeze–thaw stability, gloss, pigment binding, hold out, bond strength, and set time. Two emulsions may have the same average particle size and yet exhibit quite dissimilar behaviors because of differences in their distribution of sizes. Also, the latex particle size is a detailed blueprint of the mechanistic events present in an emulsion polymerization process. It can, therefore, be used as an effective tool for understanding polymerization mechanisms and kinetics.

A number of mathematical models have been proposed for PSD in emulsion polymerization.[1–20] Nucleation, growth, and the coalescence of the latex particles govern the evolution of the latex PSD in emulsion polymerization in general. The role of coalescence was studied separately,[21] and it was concluded that under normal reactor conditions in emulsion polymerization, particles remain stable and coalescence can be neglected. Most industrial reactors for the emulsion polymerization of conventional monomers such as styrene operate at a high level of emulsifiers, and hence, the particles are stable and do not undergo coalescence, and also, at high emulsifier levels, the dominant nucleation mechanism is micellar nucleation. A model that incorporates nucleation in micelles and growth was developed and used to study the effect of certain operating policies that would give narrow or monodisperse seed distributions.[22] It was further used to study the effects of the initial initiator charge, initial emulsifier charge, monomer addition mode (batch or semibatch), and monomer feed rates on the final PSD.[23] In this article, the model that was developed is validated against data taken from the literature. For the benefit of the readers, the model is presented again in this article.

The polymerization kinetics is based on the pseudobulk approach as opposed to the 0–1 approach. An extensive discussion on these two approaches can be found elsewhere.[24,25] Examples of models incorporating these two approaches can also be found in ref. 25. The use of pseudobulk approach obviates the need to consider a bivariate PSD with both the size and number of radicals as the internal

Correspondence to: A. Sood (sood.ashwini@rediffmail.com).

coordinates. It assumes that particles with same size have the same number of radicals. Particles having the same size may grow differently at the same time due to their different numbers of radicals. Therefore, one needs to write a population balance for the concentration of particles of size v to $v + dv$ that contain i growing radicals $[F_i(v,t)\ dv]$. Stochastic models accounting for the variation of radicals among particles of the same size and deterministic models that consider the same radical concentration (or number) for similar size particles were tested by Saidel and Katz.[26] They concluded that the deterministic model is applicable when the rate of radical arrival is much greater than its termination rate and the stochastic model is required in the case of slow radical arrival rate. It was found in a study by O'Toole[27] that the stochastic contribution to the polydispersity of latex may be neglected if the ratio of the propagation rate constant (k_p) to the termination rate constant is less than 10. If one assumes that the rate of radical entry, exit, and termination are very fast compared with the rate of particle coalescence and growth, one can neglect the variation in radical concentration among particles of same size.[28] By neglecting the effects of the stochastic broadening of the PSD that comes from the solution of the full population balance for $F_i(v,t)$, one can solve the radical balance $[i(v,t)]$ in the particle phase separately and then solve the population balance for the number concentration $[F(v,t)]$ of the particles, which assumes that similarly sized particles change their size at the same rate. Thus, the pseudobulk approach or deterministic modeling neglects the stochastic broadening in the PSD but it can account for the number of radicals greater than 1 in the particles, which is the case during the later stages of polymerization. The 0–1 approach is a widely applicable one, where the entry of a radical into a particle that already contains a radical results in instantaneous termination. As the name suggests, the 0–1 approach allows particles to contain 0 radicals or 1 radical at any given time. A necessary but not sufficient condition for the applicability of the 0–1 approach is that $i_{avg} \leq 0.5$. The 0–1 approach allows for consideration of the stochastic broadening of the PSD, but it does not allow for a number of radicals greater than 1 in the particles. It is applicable for small particles, whereas the pseudobulk is applicable for large particles. The pseudobulk approach also applies to very small particles for monomers that propagate very rapidly, such as acrylates.[24] The psuedobulk approach is preferred in modeling studies[25] and is used in this article.

The prime focus of this article is to validate the nucleation model because even after more than half of a century of commercial application of emulsion polymerization, nucleation is still not well understood.[25,29–31] Models for particle nucleation in emulsion polymerization, which are capable of predicting particle sizes and size distributions and rates with a minimum number of fitting parameters, are useful for designing recipes to give a desired outcome and to help test mechanistic hypotheses.[24] The particle nucleation stage can be manipulated to give a predesired PSD.[32] Before presenting the model, an extensive discussion on particle nucleation is provided first.

PARTICLE NUCLEATION

Nucleation refers to the formation of stable particles, which are primary sites of polymerization. In conventional emulsion polymerization, the average diameter of the original monomer droplets is about 1000–10,000 nm and that of the final latex particles is 100–300 nm. Thus, the original monomer droplets, which are an order of magnitude larger than the final latex particles, do not act as sites for nucleation. The mechanisms of particle nucleation in emulsion polymerization have been controversial. The reasons are that the small size of the initial particles (with radii < 5 nm) make them difficult to experimentally assess with transmission electron microscopy (TEM), and also, the nucleation stage is often not reproducible as it depends on a large number of factors. These factors include the emulsifier type and emulsifier concentration ([E]), the rate of radical generation, the type and concentration of electrolyte, the intensity of agitation, and many other parameters that are not easily discernible.[33] Tauer et al.[34] presented experimental results showing the influence of the reactor material and the speed of agitation on particle nucleation.

MECHANISMS OF PARTICLE NUCLEATION

Many mechanisms have been proposed for particle formation in emulsion polymerization. An exhaustive list can be found in the references cited by Coen et al.[24] and Herrera-Ordonez and Olayo.[9] The important ones are the nucleation in monomer-swollen micelles, nucleation in the aqueous phase, and nucleation in the monomer droplets. Hansen and Ugelstad[35–38] studied these nucleation mechanisms. Reviews of these mechanisms were provided by them.[39]

The micellar nucleation mechanism, postulated by Harkins[40,41] and quantified by Smith and Ewart,[42] comprises particle formation by the entry of radicals, generated in the aqueous phase, in the monomer-swollen micelles. The nucleation is over when all of the micelles have been transformed into polymer particles or have given up their monomer and emulsifier to growing particles. The Smith–Ewart model predicts the particle number accurately for styrene

and other water-insoluble monomers. The number of particles at the end of the nucleation stage is predicted to be proportional to the aqueous phase radical flux to the 0.4 power and to the initial [E] to the 0.6 power. Deviations from the Smith–Ewart model occurs when there is a substantial amount of radical exit or aqueous phase termination or when the calculation of the absorbance efficiency is in error. Deviations with respect to order from the Smith–Ewart model increase as the monomer water solubility (M_{sat}) increases.

Although the Smith–Ewart micellar nucleation model explains data for certain systems, it fails for others. This has led some authors to propose a different mechanism for nucleation. In the homogeneous nucleation theory or the nucleation in aqueous phase, the radicals generated in the aqueous phase add monomer molecules dissolved in the aqueous phase until the oligomeric radicals so formed exceed their solubility in the aqueous phase and precipitate. The precipitating radicals either nucleate a particle by adsorbing emulsifier molecules and absorbing monomer molecules or coagulate among themselves or particles already nucleated. Coagulation occurs until a critical surface potential develops to prevent further coagulation. A surface charge is presented by the initiator end groups and the emulsifier molecules. This mechanism was proposed independently by Priest[43] and Jacobi[44] and was developed further by Fitch and Tsai.[45]

Before 1952, little evidence for homogeneous nucleation existed. In 1952, Priest[43] studied the phase–phase polymerization of vinyl acetate and presented a qualitative theory for homogeneous nucleation. He concluded from experimental work that aqueous phase nucleation is important in systems with monomers that have relatively high water solubilities. Primary particle formation occurs throughout the course of the reaction. During later periods of the reaction, these primary particles coagulate with the large monomer-swollen polymer particles.

In 1968, Roe[46] developed the Smith–Ewart limiting cases for particle number from the homogeneous nucleation theory. He showed that the Smith–Ewart equation for particle nucleation was not unique to the micellar nucleation but resulted from the following assumptions: (1) nucleation stops upon the depletion of micelles, (2) the volumetric growth rate is constant, and (3) radical absorption is strictly a function of radical generation. He showed that the Smith–Ewart dependency on radical flux and surfactant concentration could be generated from homogeneous nucleation theory.

Fitch and Tsai[45] developed a quantitative theory for homogeneous nucleation. By using the collision theory for radical capture, they showed that the rate of radical capture is a function of radical generation, particle number, particle size, and diffusion distance. Primary particles may coagulate with each other because of their small size and lower surface charge. As particles coagulate, the surface-to-volume ratio decreases, which causes an increase in surface potential. When the particles become sufficiently large, coagulation ceases due to an insufficient kinetic energy to overcome the biparticle surface repulsion. Fitch and Tsai gave experimental support of this theory by polymerizing methyl methacrylate with different initiators.

Hansen and Ugelstad[35] proposed that free radicals in the aqueous phase propagate with dissolved monomer. When a critical chain length is reached, primary particles form by precipitation. During growth from a monomer radical to a primary particle, each oligomer can (1) terminate with other radicals, (2) precipitate if its length exceeds the critical chain length, or (3) be captured by a particle.

More recently, Maxwell et al.[47] suggested that the values to be used for the critical chain length are much smaller than that originally thought. They also suggested that oligomeric radical capture is independent of particle size and limited by the rate of propagation of the radical in the aqueous phase. An extensive discussion on radical entry (or capture) mechanisms was given elsewhere.[48] Prindle,[49] at the University of Wisconsin, developed a mathematical model for predicting PSD when [E] is below the critical micelle concentration (cmc) and incorporated the homogeneous–coagulative nucleation mechanism.

Tauer and Kuhn[50] developed a framework for particle nucleation on the basis of classical nucleation theory with radical polymerization kinetics and the Flory–Huggins theory of polymer solutions. The basic assumption is that waterborne oligomers form stable nuclei under critical conditions. The only adjustable parameter is the activation energy of nucleation. By means of this model, it is possible to calculate the nucleation in an unseeded emulsion polymerization with respect to the first appearance of particles. The model allows the calculation of the chain length of the nucleating oligomers, the number of chains forming one nucleus, the total number of nuclei formed, and the rate of nucleation. Further events of an emulsion polymerization, such as the coagulation or coalescence of particles, particle growth, and secondary particle nucleation, cannot be considered with this model. Tauer and Oz[51] presented experimental results that they believed contradict the micellar nucleation theory but can be explained on the basis of the previous nucleation theory.

A relatively recent development is the idea of coagulative nucleation, which may be thought of as an extension of the micellar and the homogeneous

nucleation mechanisms. According to this mechanism, proposed by Lichti et al.[52] and Feeney et al.,[53] the formation of a stable polymer particle occurs in a two-step process. The first step involves the formation of colloidally unstable precursor particles through either micellar or homogeneous nucleation. This is followed by a second step involving the coagulation of these precursor particles to form stable ''true'' or ''mature'' polymer particles. This theory is based on the positive skewness of PSD as a function of volume during interval II. This implies that the rate of nucleation during interval I increases with time until it eventually drops off as the cessation of nucleation. The authors claimed that micellar nucleation or one-step homogeneous nucleation incorrectly predicts either decreasing or constant nucleation rates.

The Sydney Group of Gilbert and Napper[54] later recognized that the apparent disqualification of the micellar mechanism in the 1980s was not definitive. This was because the observed results were also consistent with the supposition that very small particles grow slowly due to the fact that according to the Morton[55] equation, the greater the size of the particle is, the greater its monomer concentration ([M]) is. Therefore, growth by propagation in a new particle formed by micellar nucleation would also be autoaccelerating because the equilibrium of [M] increases with increasing radius. Furthermore, the Sydney Group showed that the homogeneous mechanism (ignoring coagulation) did not produce the experimentally observed number of particles in the styrene emulsion polymerization above cmc; therefore, neither could the homogeneous–coagulative mechanism. They concluded that the latter cannot be the sole mechanism responsible for particle formation above cmc and that the additional mechanism must directly involve the micelles and limited coagulation of the primary particles formed in this manner (coagulative nucleation). This hypothesis has been criticized in reference to the limited coagulation of the primary particles. Hansen[56] pointed out that it is hard to believe that completely surfactant-covered particles are sufficiently unstable to coagulate in the timescale of the reaction.

Giannetti[57] derived an extension of the homogeneous coagulative model to take into account the production of primary particles by micellar nucleation and their limited coagulation. He extended the tool, the generating function approach, that he initially developed[58] to describe the growth stage, or interval II, to describe the events during the particle nucleation stage, or interval I. He considered monotonically decreasing and monotonically increasing nucleation rate profiles and demonstrated that a positively skewed plot of the PSD also results from a monotonically decreasing nucleation rate profile as is typical of micellar nucleation. The positively skewed PSD in his treatment resulted from the stochastic broadening of the distribution as a result of a difference in radical concentrations in similar sized particles. Giannetti further attempted to generate the nucleation rate profile on the basis of the extended nucleation scheme, which incorporated the three mechanisms believed to be simultaneously participating in the formation of latex particles: micellar nucleation, homogeneous nucleation, and coagulative nucleation. The mechanistic treatment resulted in a nucleation rate profile in which the rate of nucleation initially increased and then decreased with time. This nucleation rate profile also resulted in a positively skewed PSD but the duration of the nucleation was 60–80 s, which appeared to be too low. The author was partially successful in differentiating the contributions of these three mechanisms to the overall nucleation process. He successfully showed that homogeneous nucleation did not contribute significantly to the particle formation in the presence of micelles. The author also showed that it was not necessary to include coagulative steps in the nucleation scheme to explain the positively skewed PSD. Giannetti also stated that the extension of Derjaguin-Landau-Verwey-Overbeek (DLVO) theory to model the behavior of a very small latex particle, typical of interval I, is open to discussion and implies a certain degree of arbitrariness.

Dunn[59] reported that it appeared that the micellar nucleation of latex particles of monomers with low water solubility could be consistent with the occurrence of limited coagulation or coalescence of primary particles during interval I because the rate of adsorption of surfactants on polymerizing particles is insufficient to maintain a saturated monolayer of adsorbed emulsifier on the particle surface continuously, which would mean that precursor particles become colloidally unstable periodically. Dunn[60] further reported that the initial rate of increase of the surface area of polystyrene latex particles nucleated from a micelle would result in a drop in its surface potential, which would permit a significant rate of coagulation.

Carro and Herrera-Ordonez[61] studied the number and size distribution of particles of a styrene emulsion polymerization above cmc by means of asymmetric flow-field flow fractionation (AF^4). Bimodal PSDs were obtained, which suggested that coagulation of the primary particles was not as extensive as would be expected, according to the coagulative mechanism. AF^4 allowed it them to demonstrate that the number of particles was constant during interval II.

I[21] conducted a theoretical analysis based on DLVO theory to calculate the minimum surfactant coverage required for stability against coagulation and found it to be 4.6% for two species having a hypergeometric diameter of 5 nm, which corresponded to

the micellar dimensions. The actual surfactant coverage for micelles is 100%, and hence, micelles can be considered stable against coagulation. The surfactant coverage of the particles formed from micelles, which grow as a result of polymerization and monomer transport, will not fall below 4.6% to permit coagulation. Hence, coagulation can be ruled out in the nucleation scheme above cmc.

Coen et al.[24] argued that a physically realistic model for particle formation requires one to take into account the coagulation involving very small particles. The basic reason for this is that the tiny particles, as are formed as a result of micellar and homogeneous nucleation, have highly curved double layers and are thus unstable to both heterocoagulation and homocoagulation. They noted that the predicted effect of the inclusion of coagulation on the final PSD is not large, although it is significant.

Nucleation in monomer droplets occurs when their size is reduced by homogenization and their stability is increased by the addition of an appropriate surfactant and costabilizer, which makes their total surface area large enough to compete with micelles for radicals. This was first demonstrated by Ugelstad et al.[62] at Lehigh University. Sood and Awasthi[63,64] developed and validated a mathematical model for the miniemulsion polymerization of styrene, which incorporated the full droplet size distribution and PSD. The stability of the miniemulsion droplets against degradation by molecular diffusion (or Ostwald Ripening)[65] and coagulation[21] has also been studied. Reviews of miniemulsion polymerization can be found elsewhere.[66–69]

RELATIVE IMPORTANCE OF DIFFERENT NUCLEATION MECHANISMS

Hansen and Ugelstad[39] pointed out that particle nucleation models should include all nucleation mechanisms because all of these mechanisms may compete and coexist in the same polymerization system. Hansen and Ugelstad and Song and Poehlein[70] presented probabilities for each mechanism.

It has already been pointed out that nucleation in monomer droplets can occur only when their size is reduced, which results in an increase in their total surface area. As a result, the micellar concentration will decrease as more and more emulsifier molecule is used to stabilize this increased surface area. Because of their increased surface area, the monomer droplets can compete favorably with the reduced micelle concentration for radicals. This mechanism is important in miniemulsion and microemulsion polymerization systems. With conventional emulsion polymerization (or macroemulsion polymerization), where monomer droplets are large and their total surface area is an order of magnitude less than that of micelles, nucleation in the monomer droplets can be safely neglected. Recently, Shastry and Garcia-Rubio[71,72] conducted a study to identify the most likely locus of particle nucleation in emulsion polymerization. The study provided the experimental evidence for a previously unidentified nanodroplet population in the size range 30–100 nm in diameter. To further support this experimental evidence, calculations were conducted to obtain the emulsifier distribution over the nanodroplet population. The calculation suggested the probability of the existence of the nanodroplet population to be much higher than the probability of the existence of the swollen micelles. The results, depending on the emulsification conditions, indicate the presence of about 15–80% of the dispersed phase in the nanodroplet population. The large interfacial area offered by the nanodroplet population, because of their high particle numbers and high percentage of the dispersed phase in them, makes them the most probable particle nucleation loci in the emulsion polymerization processes. Designed experiments were performed to experimentally observe the changes in the nanodroplet population. The effects of process variables, namely, pH, surfactant concentration and temperature, on the size and compositional characteristics of the nanodroplet population were investigated. The results suggested that the surfactant-to-oil ratio was the dominating factor governing the size and weight percentage of the dispersed phase in the nanodroplet population.

The relative importance of homogeneous and micellar nucleation mechanisms depends strongly on the water solubility of the monomer and [E] in the aqueous phase. Monomers with high water solubility will exhibit a relatively high rate of homogeneous nucleation because of the high rate at which radicals can add monomer molecules in the aqueous phase. The probability of homogeneous nucleation will also increase with decreasing emulsifier level ([E]), as growing radicals will precipitate before they are captured by the micelles. The homogeneous nucleation mechanism is considered the dominant mechanism for particle nucleation when [E] is below cmc or in emulsifier-free emulsion polymerization systems. High [E]s and less water-soluble monomers will favor micellar nucleation. Schlueter[73] showed experimentally that the homogeneous nucleation mechanism was effective in a persulfate-initiated polymerization system, even for monomers of low water solubility, such as styrene and butadiene, and [E] above cmc. With catalyzed agglomeration, the particle size, monodispersity coefficient, and particle formation time were investigated as a function of monovalent cation concentration, [E], and polymerization temperature. All correlations found were either consistent with homogeneous nucleation or

completely excluded micellar nucleation. Varela de la Rosa et al.[74] reported a reaction rate profile, measured through calorimetry, for styrene emulsion polymerization above cmc, which showed a maximum in interval II. It was believed so far that in interval II, the reaction rate was constant. They attributed this maximum in the rate profile to homogeneous nucleation, which led to an increase in the number of particles formed after the disappearance of micelles. Varela de la Rosa et al. reported that there was a formation of polymer particles up to 40% conversion; that is, the number of particles increased during interval II instead of remaining constant, as would be expected according to classical behavior. They made their particle size measurements with the capillary hydrodynamic fractionation technique. For some of the samples, TEM was used, which assumed for the calculations the same diameter ranges obtained from the capillary hydrodynamic fractionation distributions. This behavior contrasted with that reported by Harada et al.[75] in the early 1970s for the same system and conditions. Harada et al. reported that the number of particles (obtained by TEM) was constant during interval II (both Varela de la Rosa et al. and Harada et al. determined the limits of intervals I and II by measuring surface tension on samples taken during the course of the polymerization). Varela de la Rosa et al. proposed that particle formation during interval I is dominated by micellar nucleation whereas, in interval II (which they called stage II), the particles formed are produced by homogeneous nucleation. Herrera-Ordonez and Olayo[9,10] developed a mathematical model for the prediction of PSD in styrene emulsion polymerization above cmc. They considered both the micellar and homogeneous nucleation mechanisms. They reported that the contribution of the homogeneous nucleation mechanism to the number of particles formed was insignificant compared to that of micellar nucleation. They further reported that the maximum seen in the rate of nucleation profile by Varela de la Rosa et al. could be attributed to the increase in the average number of radicals in the particles with particle size. Furthermore, the experimental results of Carro and Herrera-Ordonez[61] allowed it to be demonstrated that the number of particles is constant during interval II. The same was reported earlier by Harada et al.[75]

This model incorporates micellar nucleation only. The treatments of Giannetti[57] and Herrera-Ordonez and Olayo[9,10] showed that homogeneous nucleation does not contribute significantly above cmc for a sparingly water-soluble monomer such as styrene. Hence, homogeneous nucleation is not included in this model. Coagulation is also not included in this model. Carro and Herrera-Ordonez's[61] work on a styrene emulsion polymerization above cmc by means of AF[4] suggested that coagulation of the primary particles was not as extensive as would be expected according to the coagulative mechanism. My own theoretical work[21] based on DLVO theory to calculate the minimum surfactant coverage required for stability against coagulation showed it to be 4.6% for two species having a hypergeometric diameter of 5 nm, which corresponds to the micellar dimensions. The actual surfactant coverage for micelles is 100%, and hence, micelles can be considered stable against coagulation. The surfactant coverage of the particles formed from micelles, which grow as a result of polymerization and monomer transport, will not fall below 4.6% to permit coagulation. Hence, coagulation can be ruled out in the nucleation scheme above cmc. Although the works of Shastry and Garcia-Rubio[71,72] have shown that nucleation in small monomer droplets is dominant even in the presence of micelles, droplet nucleation is not included in this model.

MODEL DEVELOPMENT

Emulsion polymerization follows the kinetics of free-radical-initiated vinyl addition polymerization superimposed on the heterogeneous colloidal latex system. A typical emulsion polymerization reactor, therefore, consists of many components and phases undergoing numerous chemical reactions and mass-transfer processes simultaneously and with strong interactions. The important physical and chemical events in emulsion polymerization include radical generation; particle nucleation; chain propagation; chain termination; the mass transfer of radicals, monomer(s), and emulsifier(s) to and from the latex particles; particle coalescence; and the variation of the termination rate constant and k_p with conversion. A general modeling framework, incorporating all the relevant mechanisms can be very complex. Such a framework consists of a population balance equation that accounts for the change in the number of particles of a given size due to growth and coalescence. The nucleation term provides the boundary condition for this infinite-order partial differential/integral equation system and accounts for the change in the number of particles at the boundary or the initial micellar size. These equations are coupled to the phenomena occurring in the various phases: the particles, the droplets, and the aqueous phase. This coupling is represented in terms of the overall reactor balances for the reactor volume, aqueous phase, monomer, polymer, initiator, emulsifier, and electrolyte; aqueous phase balances for the monomer, micelles, and radicals; equations describing [M] inside the particle and the number of radicals inside the particle, which together give the rate of particle

mass growth (R_g); the nucleation rate, which in general, includes all of the different nucleation mechanisms, such as micellar, homogeneous, and coagulative, in monomer droplets; and the coagulation rate. The resulting system of equations to be solved consists of partial differential/integral equations, coupled ordinary differential equations, nonlinear algebraic equations, and Bessel functions. The solution of such a model poses a challenge to any model developer. The approach that I followed consisted of modeling and solving special cases relevant to a given emulsion polymerization system. If coalescence is negleted, the population balance model reduced from a system of partial differential/integral equations to a system of partial differential equations. This system of equation was solved with orthogonal collocation. Details of this method and its extension to orthogonal collocation on finite elements was given in an earlier article.[20]

PHYSICAL PICTURE

The model simulates an isothermal, well-stirred, semibatch emulsion polymerization reactor. Polymer particles, formed through micellar nucleation or present as seed, act as the site of polymerization. The monomer is partitioned among the aqueous phase, particle phase, and monomer droplets; its concentration in the particle phase is determined by the thermodynamic balance among these phases. The net flux of radicals to the growing particles, determined by the rate of radical entry into, termination inside, and exit from the particles, determines the average number of radicals in them. [M] and the average number of radicals within a particle determine its growth rate. The emulsifier stabilizes the growing particle surface. [E] in the reactor determines the nucleation of new particles. When present above cmc and that concentration required to stabilize the existing particle surface, the emulsifier forms micelles, which act as a site for nucleation. Differences in the nucleation times and growth rates of the various particles results in differences in their sizes and determines the average size and broadness of the resulting PSD.

OVERALL REACTOR BALANCES

The overall reactor balances include the balances for [M], polymer concentration ([P]), [E], and initiator concentration ([I]) and balances for the volume of the reaction mixture (V_R) and the volume of the aqueous phase (V_W). The material balances, which express the rate of change of moles of each of the species, contain accumulation and reaction terms (where appropriate). V_R changes because of density differences between the monomer and the polymer.

$$\frac{d[\mathrm{M}]_R V_R}{dt} = Q_M[\mathrm{M}]_f - R_p V_R \tag{1}$$

$$\frac{d[P]_R V_R}{dt} = R_p V_R \tag{2}$$

where R_p is the rate of polymerization and is calculated by the following equation:

$$R_p = k_p \frac{\rho_M}{\mathrm{MW}_M} \int_{V_M}^{\infty} F(v,t)\Phi i \, dv$$

$$\frac{d[\mathrm{E}]_R V_R}{dt} = Q_E[\mathrm{E}]_f \tag{3}$$

$$\frac{d[\mathrm{I}]V_W}{dt} = Q_I[\mathrm{I}]_f - k_d[\mathrm{I}]V_W \tag{4}$$

$$\frac{dV_R}{dt} = Q_M + Q_E + Q_I - \left(\frac{1}{\rho_M} - \frac{1}{\rho_p}\right) R_p \mathrm{MW}_M V_R \tag{5}$$

$$\frac{dV_W}{dt} = Q_E + Q_I \tag{6}$$

where Q_M, Q_E, and Q_I are the volumetric flow rates of the monomer, emulsifier, and initiator; $[\mathrm{M}]_R$ is the monomer concentration in the reactor; $[P]_R$ is the polymer concentration in the reactor; $[\mathrm{E}]_R$ is the emulsifier concentration in the reactor; $[\mathrm{E}]_f$ is the emulsifier concentration in the feed; $[\mathrm{I}]_f$ is the initiator concentration in the feed; $[\mathrm{M}]_f$ is the monomer concentration in the feed; $F(v,t)$ is the number density of the particles; k_d is the initiator decomposition constant; ρ_M is the density of the monomer; ρ_P is the density of the polymer; Φ is the monomer volume fraction in the particle; i is the average number of radicals in the particle; MW_M is the molecular weight of the monomer; and V_M is the volume of the micelle.

AQUEOUS PHASE BALANCES

Aqueous phase balances involve the balance for the radical, micelles, and dissolved monomer.

Equation (7) combines the rates of radical generation in the aqueous phase, termination in the aqueous phase, entry into the particles, entry into the micelles, and exit from the particles. A quasi-steady-state assumption is used for radical balance:

$$2fk_d[\mathrm{I}]V_W - k_{tw}[\mathrm{R}]^2 V_W - 4\pi k_{mp}[\mathrm{R}]N_a \int_{V_m}^{\infty} F(v,t)V_R r^n dv$$

$$- 4\pi k_{mm} r_m^n [\mathrm{R}]N_a[\mathrm{m}]V_W + \int_{V_m}^{\infty} k_{de}(v)F(v,t)V_R i dv = 0 \tag{7}$$

where f is the initiator efficiency, [R] is the aqueous phase radical concentration, N_a is Avogadro's number, r is the radius of the particle, k_{tw} is the aqueous phase radical termination constant, k_{mp} is the radical entry rate coefficient in the particle, k_{mm} is the radical entry rate coefficient in the micelle, [m] is the micelle concentration in the reactor, k_{de} is the radical exit rate coefficient, and n is the exponent that determines whether radical capture is propagation-, diffusion-, or collision-controlled.

The emulsifier distributes itself among the particle surface, monomer droplets, and the aqueous phase. In conventional emulsion polymerization, where the total surface area of monomer droplets is an order of magnitude less than the micelles initially and decreases further as polymerization progresses, the amount of emulsifier adsorbed on the monomer droplet can be neglected. The free emulsifier in the aqueous phase ($[E]_W$), which is the amount of emulsifier in the aqueous phase in excess of that required to stabilize the growing particle surface [total particle surface area (A_P)], and that dissolved in the aqueous phase [emulsifier critical micelle concentration ($[E]_{cmc}$)] forms the micelles. The following equations represent the micellar balance:

$$[m] = 0 \quad \text{if } [E]_W \leq [E]_{cmc} \tag{8}$$

Otherwise

$$[m] = \left([E]_W - [E]_{cmc}\right) \frac{MW_E N_a a_{em}}{4\pi {r_m}^2}$$

where

$$[E]_W V_W = [E]_R V_R - \frac{A_P}{a_{ep} N_a}$$

$$A_P = 4\pi \int_{V_M}^{\infty} F(v,t) V_R r^2 \, dv$$

where MW_E is the molecular weight of the emulsifier, a_{em} is the emulsifier coverage area on a micelle, r_m is the radius of the micelle, a_{ep} is the emulsifier coverage area on a particle, and V is the volume of the particle.

The amount of monomer dissolved in the aqueous phase ($[M]_W V_W$, where $[M]_W$ is the monomer concentration in the aqueous phase) is obtained by the difference between the total amount of monomer in the reactor ($[M]_R V_R$) and the monomer present inside the particles and the monomer droplets ($[M]_D V_D$, where $[M]_D$ is the monomer concentration in the droplet phase and V_D is the volume of the monomer droplets):

$$[M]_W V_W = [M]_R V_R - \frac{\rho_M N_a}{MW_M} \int_{V_M}^{\infty} F(v,t) V_R v \Phi \, dv - [M]_D V_D \tag{9}$$

POPULATION BALANCE EQUATION

The population balance equation, expressed in terms of the mass of the polymer in the particle (m_p) as the size variable, without the coalescence term is given by

$$\frac{\partial \left[F\left(m_p,t\right)V_R\right]}{\partial t} + \frac{\partial \left[R_g F\left(m_p,t\right)V_R\right]}{\partial m_p} = 0 \tag{10}$$

The boundary condition is

$$\frac{\partial \left[F\left(m_p,t\right)V_R\right]}{\partial t} = R_n(t)$$

where R_n is the rate of micellar nucleation. The initial condition is

$$F(m_p, 0) = 0$$

The previous equation uses m_p as the internal coordinate. Rewriting the population balance with the birth time (t') as an internal coordinate, one obtains

$$\frac{\partial \left[F\left(t',t\right)V_R\right]}{\partial t} = 0; \quad F\left(t',t\right)V_R/t' = R_n\left(t'\right) \tag{11}$$

Although the t' and m_p descriptions are mathematically equivalent, [$F(v,t) = F(m_p,t) = F(t',t)$], the t' description is computationally more attractive. If the problem is formulated with t', the divergence term vanishes, and therefore, eq. (11) has the solution:

$$F\left(t',t\right)V_R = R_n\left(t'\right) \tag{12}$$

The evaluation of the rate of particle nucleation (R_n) and the evaluation of R_g are discussed later.

MICELLAR NUCLEATION

R_n is given by the rate of radical capture by micelles (R_{em}). Radical entry into the micelles (and latex particles) has been postulated to take place via different mechanisms, with the important ones being radical entry due to propagation in the aqueous phase, radical entry due to diffusion, and radical entry due to collision. In this article, R_{em} is given as

$$R_{em} = k_{mm} 4\pi \left(r_m\right)^n [R] N_a [m] V_W \tag{13}$$

The choice of $n = 0$ gives the propagational entry model, $n = 1$ gives the diffusion model for entry, and $n = 2$ gives the collision model. The rate of radical entry is coupled to the aqueous phase radical balance, which is given by eq. (7).

By neglecting the aqueous phase termination and solving the resulting equation for [R], one obtains

$$[\mathrm{R}] = \frac{2fk_d[\mathrm{I}]V_W + \int_{V_M}^{\infty} k_{de}(v)F(v,t)V_R i(v)\,dv}{4\pi k_{mm}(r_m)^n[\mathrm{m}]N_a V_W + 4\pi k_{mp}\int_{V_M}^{\infty} F(v,t)V_R r^n\,dv} \tag{14}$$

By substituting [R] from eq. (14) into eq. (13), one obtains the expression used in these simulation studies for R_n:

$$R_n = 4\pi k_{mm}(r_m)^n[\mathrm{m}]N_a V_W \times \frac{2fk_d[\mathrm{I}]V_W + \int_{V_M}^{\infty} k_{de}(v)F(v,t)V_R i(v)\,dv}{4\pi k_{mm}(r_m)^n[\mathrm{m}]N_a V_W + 4\pi k_{mp}\int_{V_M}^{\infty} F(v,t)V_R r^n\,dv} \tag{15}$$

This is the model for micellar nucleation.

PARTICLE GROWTH

R_g is given by eq. (16), which defines the rate of the reaction (g of polymer/s) in a particle having i number of radicals and the monomer volume fraction, Φ:

$$R_g \equiv \frac{dm_p}{dt} = \frac{k_p i \Phi \rho_M}{N_a} \tag{16}$$

The volume of the monomer swollen latex particle (v) can be related to m_p in it by:

$$v = \frac{m_p}{\rho_P(1-\Phi)} \tag{16a}$$

The two equations, which together give the volume of the latex particle at any time, contain two variables, Φ and i. The evaluation of these variables is discussed in the following sections.

MONOMER VOLUME FRACTION IN THE PARTICLE

Monomer diffusion into the polymer particles ordinarily occurs at fast rate.[76,77] Thus, one can make the quasi-steady-state assumption that the [M] inside the particles is at its equilibrium value at all times. The equilibrium [M] can be obtained from eq. (17), given by Min and Ray,[19,20] which is an extension of that developed by Morton et al.:[55]

$$\frac{2\gamma \mathrm{MW}_M}{r\rho_M R_G T} + \left[1 - \Phi + \ln\Phi - \chi(1-\Phi)^2\right] = \ln\left(\frac{[\mathrm{M}]_w}{[\mathrm{M}]_{\mathrm{sat}}}\right) \tag{17}$$

where γ is the interfacial tension, R_G is the universal gas constant, T is the absolute temperature, χ is the Flory–Huggins interaction parameter, and $[\mathrm{M}]_{\mathrm{sat}}$ is the monomer concentration at saturation in the aqueous phase.

The previous equation results from the balance between the gain in free energy caused by the increase in the interfacial area on swelling, the loss in free energy caused by the mixing of the monomer with the polymer, and the gain in free energy caused by the separation of monomer from the aqueous phase. This equation is coupled to the monomer balance because of the presence of monomer in the aqueous phase. $[\mathrm{M}]_W$ can be determined with eq. (9).

When monomer droplets are present in the reactor, the aqueous phase is saturated ($[\mathrm{M}]_W = [\mathrm{M}]_{\mathrm{sat}}$). Then, Φ can be calculated from eq. (17); however, when the monomer droplets are absent ($[\mathrm{M}]_D = 0$), eqs. (9) and (17) must be solved simultaneously for Φ and $[\mathrm{M}]_W$. One can make an important simplification by neglecting the first term in eq. (17), which accounts for the gain in the free energy caused by an increase in the interfacial area on swelling. This simplification enables one to compute Φ independently of particle size. This results in a great computational advantage, as now the two equations need not be solved for different values of r at each integration step. By combining eqs. (9) and (17), one obtains

$$[\mathrm{M}]_{\mathrm{sat}}V_W \exp\left[1 - \Phi + \ln\Phi + \chi(1-\Phi)^2\right] - [\mathrm{M}]_R V_R - [\mathrm{M}]V_P = 0 \tag{18}$$

where $[\mathrm{M}]_P$ is the monomer concentration in the particle phase and V_P is the volume of the polymer. This equation can be solved for Φ for given values of V_W, $[\mathrm{M}]_R V_R$, and $[\mathrm{M}]_P V_P$ (which can be obtained by the solution of the overall reactor balances for the aqueous phase, monomer, and polymer).

AVERAGE NUMBER OF RADICALS PER PARTICLE

The average number of radicals per particle is determined by the rate of radical entry into, exit from, and termination inside the particle. This is given by a quasi-steady-state equation, which is the Smith–Ewart recursion relation:[42]

$$k_e[F_{i-1}(v,t) - F_i(v,t)] + k_{de}[(i+1)F_{i+1}(v,t) - iF_i(v,t)] + \frac{k_t}{2vN_a}[(i+2)(i+1)F_{i+2}(v,t) - i(i-1)F_i(v,t)] = 0 \tag{19}$$

where k_e is the radical entry rate coefficient and k_t is the radical termination rate constant inside the particle.

In the Stockmayer–O'Toole[78,79] form of this equation, the average number of radicals per particle [$i(v,t)$] is given by

$$i(v,t) = \sum_{i=0}^{\infty} \frac{iF_i}{F(v,t)} = \frac{a}{4}\frac{I_b(a)}{I_{b-1}(a)} \tag{20}$$

where $I_b(a)$ is the modified Bessel function of the first kind of order b and argument a and

$$a = 4\left(\frac{vN_a k_e}{k_t}\right)^{1/2}$$

$$b = \frac{2vN_a k_{de}}{k_t}$$

where parameter a accounts for the relative importance of radical entry with respect to radical termination and parameter b accounts for the relative importance of radical exit with respect to radical termination inside the particle.

For this article, the continued fraction form, first used by Ugelstad et al.,[80] is used

$$i = \frac{a}{4}\frac{I_b(a)}{I_{b-1}(a)} = \frac{1}{2}\frac{a^2/4}{b+}\frac{a^2/4}{b+1+}\frac{a^2/4}{b+2+} \tag{21}$$

MODEL SOLUTION

The mathematical framework consists of the population balance equation, which is a hyperbolic partial differential equation. The model also contains simultaneous ordinary differential equation representing the overall reactor balances, algebraic equations representing the aqueous phase balances and the monomer partitioning among different phases, and Bessel functions representing the average number of radicals inside the particle. Efficient numerical methods are needed to solve the previous system of equations.

An efficient method is needed to solve the population balance equation. Especially important is the efficient integration of the total particle distribution to obtain an accurate evaluation of terms such as A_P and the reaction rate without the investment of large amounts of computer time and storage. The numerical technique that seems the best for the solution of the population balance equation is orthogonal collocation. This method was considered in detail in a previous article.[64]

NUMERICAL IMPLEMENTATION

IMSL MATH/LIBRARY version 1.1 Fortran subroutines (Absoft Corporation, Rochester Hills, MI) were used to numerically solve the modeling equations. Subroutine IVPAG, which is based on the gear method, was used to solve the initial value ordinary differential equations; subroutine ZREAL, which uses the Muller method, was used to solve the nonlinear algebraic equation to obtain the value of Φ. As already stated, the continued fraction form developed by Ugelstad et al. was used to evaluate the average number of radicals inside the particles.

MODEL PARAMETERS

Emulsion polymerization models involve a large number of parameters. These parameters relate to the physicochemical and kinetic properties of reaction ingredients, which are primarily the monomer, polymer, emulsifier, and initiator. For these simulations, the system that was chosen included styrene (monomer), potassium persulfate (initiator), and sodium dodecyl sulfate (emulsifier). Styrene is a relatively water-insoluble monomer, potassium persulfate is a dissociative initiator, and sodium dodecyl sulfate is an anionic emulsifier. In the following paragraphs, I emphasize that although this is a simple and a fairly common system that has been used in many kinetic investigations, complete and unambiguous values of the various parameters were not available in the open literature. The parameters that were not subject to speculation and that were readily available from standard references were ρ_M and ρ_P, M_{sat}, the equilibrium monomer volume fraction (Φ_{sat}), MW_M, MW_E, and the molecular weight of the initiator (MW_I).

The parameters whose values were subject to speculation included k_p; the parameters that defined the emulsifier characteristics, namely, the area occupied by the emulsifier molecule on a micelle and on a particle (a_{em} and a_{ep}), respectively; $[E]_{cmc}$; r_m; and the parameters that defined the initiator characteristics, namely, k_d and f.

Besides these parameters, there were parameters describing events such as radical entry into the particles, radical exit from the particles, and the variation of k_p and the termination rate constant with conversion (gel effect).

The values of k_p for styrene at 50°C, as reported in the *Polymer Handbook*,[81] are 206,000, 209,000, 223,000, and 309,000 cm^3/mol s, depending on the source from which they are taken. These vary from one another by 35%. The value obtained with the expression $1.8 \times 10^{12} \exp(-10{,}400/R_gT)$, presented by Rawlings and Ray,[14] which they obtained by fitting the values presented in the *Polymer Handbook* with the Arrhenius expression was 163,775 cm^3/mol s. Similarly, the uncertainty in the value of $[E]_{cmc}$ required some attention; the published values of $[E]_{cmc}$ for sodium dodecyl sulfate are found to vary from 0.001 to 0.009*M*, depending not only on the method of determination (e.g., surface tension or conductance mea-

surements) but also on the purity and the source of the samples.[82] Similarly, there were discrepancies in the literature values of a_{ep}, k_d, and f.

It has been emphasized[83] that the rate coefficients used for emulsion polymerization studies should be obtained from extensive sets of experiments on an emulsion polymerization system, so that uncertainties in or variation from kinetic data obtained from other studies (e.g., bulk polymerization) are obviated. This approach was followed in this study, in which simulations were validated against the experimental data of Harada et al.[75] Harada et al. calculated the values of k_p, k_df, and the areas occupied by the emulsifier molecule (a_{em} and a_{ep}) from the experimental values of the constant rate during interval II, the number average degree of polymerization, and the proportionality constant relating the number of particles formed to [E], respectively. The value of k_p was 212,000 cm^3 mol^{-1} s^{-1} (at 50°C). This value agreed well with the previously reported value of 209,000 cm^3 mol^{-1} s^{-1} (at 50°C).[84] Similarly, the calculated value of k_df of 0.665×10^{-6} s^{-1} (at 50°C) agreed well with the value of the persulfate rate constant given in the literature[85] ($k_d = 0.15 \times 10^{-5}$ s^{-1} and $f = 0.5$). The value of a_{ep} (and a_{em}) calculated by Harada et al. was 35×10^{-16} cm^2/molecule, which agreed approximately with the literature values for adsorption at the oil–water interface of 45–50 $\times 10^{-16}$ cm^2/molecule. The authors also reported the measured values of $[E]_{cmc}$ to be 0.50 g/L at 50°C. In this study, the values of k_p, a_{ep} (and a_{em}), and $[E]_{cmc}$ as calculated by Harada et al. were used. The value of f was set at 0.5, and the value of k_d was the value obtained from the literature.[85]

The mechanism of radical entry is one of several mechanisms in emulsion polymerization for which there exists several models that are mutually contradictory. For the prediction of full PSD, one not only needs the accurate numerical values of the coefficients for radical entry but also the correct particle size dependency of these coefficients. Plausible arguments have been given to identify the correct model for radical entry into the particles and the micelles.[48,64] The collision entry model, for which $n = 2$, was chosen as the radical entry model. In this simulation study, the following expression for the radical exit, used by Rawlings and Ray,[14] was initially used:

$$k_{de} = (3D_m k_{trm}/k_p)/(D_m \mathrm{MW}_M/\rho_M k_p \Phi + r^2) \qquad (22)$$

where D_m is the effective diffusivity of the radical and k_{trm} is the coefficient of chain transfer to the monomer. The results given here are for $k_{de} = 0$.

The increase in the polymerization rate with increased monomer conversion is well known and is called the *gel effect*. The increase in the reaction rate is due to diffusional limitations causing a decrease in k_t. At a sufficiently high conversion, k_p also decreases. The gel effect correlations available in the literature are empirical or semiempirical in nature. In this study, the gel effect was not included, as most of the experimental data (except at high conversions for some cases) could be explained without including it. Table I lists the values of the various parameters used in this work and the references from which they were taken.

TABLE I
Values of Various Parameters Used in the Simulations

	Reference source
Styrene	
$\mathrm{MW}_M = 104.15$ g/g mol	86
$\rho_M = 0.906$ g/cm^3	86
$\rho_P = 1.04$ g/cm^3	87
$\Phi_{sat} = 0.6$	88
$M_{sat} = 2.6 \times 10^{-6}$ g mol/cm^3	20
$k_p = 212{,}000$ cm^3 g mol^{-1} s^{-1} (at 50°C)	75
$k_t = 6.52 \times 10^{16} \exp(-8870/R_GT)$ cm^3 g mol^{-1} s^{-1}	13
$k_{trm} = 7.0 \times 10^{-5} k_p$	13
$D_m = 7.1 \times 10^{-11}$ cm^2/s	13
Sodium dodecyl sulfate	
$\mathrm{MW}_E = 270.33$ g g mol^{-1}	
$[E]_{cmc} = 0.0005$ g/cm^3 (at 50°C)	75
$r_m = 2.5 \times 10^{-7}$ cm	20
$a_{em} = a_{ep} = 35 \times 10^{-16}$ cm^2/molecule	75
Potassium persulfate	
$\mathrm{MW}_I = 270.33$ g g mol^{-1}	89
$k_d = 1.8 \times 10^{17} \exp(-34{,}100/R_GT)$ s^{-1}	85
$f = 0.5$	
This study	
$n = 2$	
$\varepsilon = 0.08$	
$k_{de} = 0$	

MODELING ASSUMPTIONS

A number of assumptions were made while I was developing the model. The purpose of this section is to emphasize the motivation behind these assumptions and also to point out cases where these assumptions may or may not be applicable.

Some of these assumptions are well established and are normally invoked when one describes emulsion polymerization. These include the following:

1. I assumed that the particle phase was the predominant locus of polymerization. It is generally accepted that in emulsion polymerization systems, almost all of the polymer is formed within the latex particles, except for monomers such as acrylonitrile, which do not appreciably swell their polymer.[83]
2. I made quasi-steady-state assumptions for the radical concentrations in the aqueous phase and the particle phase. Min and Ray[20] emphasized

the need to make the quasi-steady-state assumptions for the radical concentrations in both the particle and the aqueous phase. There are a large variety of timescales in the reactor, ranging form about 1 s for free-radical dynamics to several hours for polymerization to high monomer conversion. The quasi-steady assumption, where it is assumed that the radicals in both phases adjust their populations in a timescale that is small compared to other changes (e.g., that for particle growth), largely relieve the stiffness of the modeling equations. Exceptions to these assumptions might occur where there is a large gel effect that leads to a very high R_g, in the very early stages of the reaction, or when the initiation suddenly ceases, as can be brought about when γ-relaxation experiments are used.[83]

3. I assumed that rate constants were not dependent on the radical chain length. Maxwell et al.[47] emphasized the need to make a distinction between the rate constants for the initial propagation step and the subsequent propagation steps. The rate constant for the initial propagation step, which occurs between an initiator radical and monomer unit, is considered to be many orders greater that that for the propagation reaction between a macroradical and a monomer unit. This difference will occur, as the authors postulated, because the initiator radical is charged and will have stronger affinity for the monomer unit, and also, the presence of a long chain macroradical reduces the rate at which a monomer can achieve correct orientation with respect to the macroradical for the reaction. For similar reasons, it was argued[83] that one needs to distinguish between the exited monomeric radical from the particle and the initiator radical. Distinguishing between these radicals requires the incorporation of individual balances for the various radicals. These microscopic details were neglected in this model.
4. I assumed that chain transfer to a small molecule (e.g., monomer unit) could only lead to radical exit. Polymerizing radical oligomers of any significant molecular weight are not expected to transfer from the particles to the aqueous phase. Such molecules would normally be strongly hydrophobic and perhaps entangled with polymer molecules in the particles.[90]

There were other assumptions made to ease the computational effort and keep the model mathematically tractable. These include:

1. Particle coalescence was considered negligible. It was emphasized that during emulsion polymerization operation, enough care was taken to reduce coalescence. However, under certain conditions, coalescence of dispersed entities can occur at various stages during emulsion polymerization and influence mechanisms such as particle nucleation and growth. The nucleation process might involve the coagulation of precursor entities to form polymer particles.[52,91] Feeney et al.[53] detected the precursor species using small-angle neutron scattering by halting the coagulation process in a gelatinous medium. Growth and coalescence can be competitive rate processes. Some models of emulsion polymerization work well only when particle coalescence is included, especially those that apply to the emulsion polymerization of vinyl chloride.[92]
2. Micellar nucleation was assumed to be the mechanism for particle formation above cmc for monomers of low water solubility. The reasons I considered only the micellar nucleation mechanism were given earlier.
3. It was assumed that the contribution of stochastic broadening to the PSD could be neglected. Before solving the bivariate distribution accounting for the variation or radical concentration among similar sized particles and thereby increasing the computational effort, it is important to access the contribution of stochastic broadening to the PSD. It was documented[93] that if one starts with a monodisperse seed and conditions are created so as to avoid particle coagulation or the generation of new particles, one ends with a monodisperse final PSD, which thereby gives evidence that stochastic broadening does not contribute significantly to the broadening of the PSD.
4. I assumed that Φ was not dependent on the particle size and γ. It was shown through simulations that Φ was insensitive to the particle size and γ, except at low particle sizes.[94] To account for these effects, one should not only account for the variation in particle size but also the variation in γ that occurs during the course of a reaction, as has been monitored.[95] γ increases as the particle size increases because the adsorbed emulsifier is less effective in stabilizing the growing surface. The effects of variations in γ and particle size (r), on Φ are self-compensating as $\Phi = f(\gamma/r)$, and therefore, it can be safely assumed that these variations will not effect Φ significantly during the reaction.
5. I assumed that radical termination in the aqueous phase could be neglected. Nomura[96] showed, through calculations for typical reaction conditions, that the average residence time for a radical to be in the water phase before it enters a particle is about 10^{-5} s, whereas the

TABLE II
Comparison of N_P^{exp} and N_P^{mod}

[E] (g/L of water)	N_P^{exp} (particles/cc of water)	N_P^{mod} (particles/cc of water)
1.88	1.8×10^{14}	1.76×10^{14}
3.13	2.2×10^{14}	2.61×10^{14}
6.25	4.0×10^{14}	4.17×10^{14}
12.50	6.0×10^{14}	6.49×10^{14}
25.00	10.0×10^{14}	9.97×10^{14}

N_P^{exp} = experimental value of the total number of particles formed; N_P^{mod} = predicted value of the total number of particles formed.

average time needed for a radical to be deactivated by a termination reaction in the aqueous phase is about 10^3 s. Thus, radical entry is greatly favored over radical termination. Through similar calculations, Maxwell et al.[47] also showed that radical entry is favored over radical termination in the aqueous phase. A criterion for neglecting aqueous phase termination was developed.[64]

Some of these assumptions restrict the model's range of application. When emulsion polymerization is described where the emulsifier is present below cmc or when the emulsifier is absent (emulsifier-free emulsion polymerization), phenomena such as particle coalescence, homogeneous nucleation, and termination in the aqueous phase need to be considered. This model is applicable to emulsion polymerization systems where the emulsifier is present above cmc.

VALIDATION APPROACH

As already stated, the system selected included styrene (monomer), sodium dodecyl sulfate (emulsifier). and potassium persulfate (initiator). The experimental data of Harada et al.[75] was chosen for the purpose of validating the dynamic simulations for two main reasons. First, the authors reported the values of the important parameters such as k_p, the area occupied per emulsifier molecule, and so on, as calculated from their experimental results. These values could be used directly for the simulations without any ambiguity about their accuracy. Second, the authors reported the values of a number of variables, which included the total number of particles formed (N_P), duration of the nucleation period (t_n), conversion at the end of nucleation, variation of Φ with time, and conversion–time curves for different monomer, initiator, and emulsifier amounts. All of the experiments were run at 50°C.

Defining ε as the ratio of the entry coefficient of the radical entry into micelles to that into particles ($\varepsilon = k_{mm}/k_{mp}$) where ε physically defines the difficulty in radical entry into micelles relative to that into particles, the value of ε was varied from 1 to 0 and adjusted to give a close match between the experimentally reported value for N_P at one of the runs that corresponded to [M], [I], and [E] values of 0.5 g/cc (water), 1.25 g/L (water), and 25.0 g/L (water), respectively. The value $\varepsilon = 0.08$ gave the best results. The value of ε was kept constant for all of the simulations. The values of all of the remaining parameters were kept the same, as reported in Table I. No effort was made to vary any of the values to fine tune the predicted values to the experimentally reported values. Tables II–IV show the comparison between the predicted values and the experimentally reported values for N_P, t_n, and the conversion at the end of the nucleation period (X_n). We concluded from these results that the predicted values were in close quantitative agreement with the experimental values. These parameters help characterize the nucleation stage. As concluded, the micellar nucleation model used in this study was reliable.

Harada et al.[75] also measured and reported the variation of Φ with conversion (X) for three different [E]s while keeping [I] and [M] constant. Figure 1 compares the model predictions (dotted line) for the aforementioned variation and the experimentally reported variation. The authors observed that for different emulsifier levels, the value of Φ was nearly constant in the range when X was less than 0.43 and in the range when X was greater than 0.43, the variation of Φ with X can be expressed as $\Phi = (1 - X)$.

TABLE III
Comparison of t_n^{exp} and t_n^{mod}

[E] (g/L of water)	t_n^{exp} (min)	t_n^{mod} (min)
1.88	—	3.67
3.13	5.1	5.39
6.25	9.2	8.59
12.50	12.5	13.36
25.00	18.0	19.45

t_n^{exp} = experimental value of the duration of the nucleation period; t_n^{mod} = predicted value of the duration of the nucleation period.

TABLE IV
Comparison of X_n^{exp} and X_n^{mod}

[E] (g/L of water)	X_n^{exp}	X_n^{mod}
1.88	—	0.005
3.13	0.005	0.012
6.25	0.03	0.030
12.50	0.06	0.073
25.00	0.146	0.173

X_n^{exp} = experimental value of the conversion at the end of the nucleation period; X_n^{mod} = predicted value of the conversion at the end of the nucleation period.

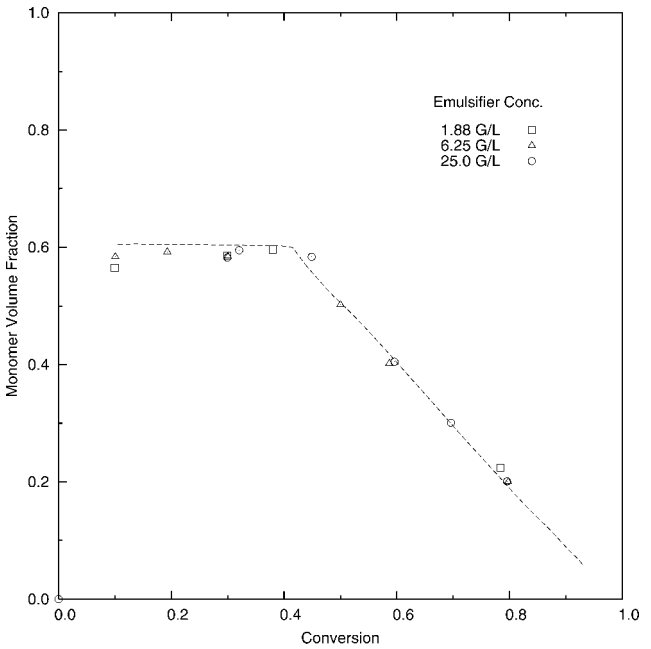

Figure 1 Comparison of the model prediction and experimental data[75] for the variation of Φ's with the conversion ([I] = 1.25 g/L, [M] = 0.5 g/cc).

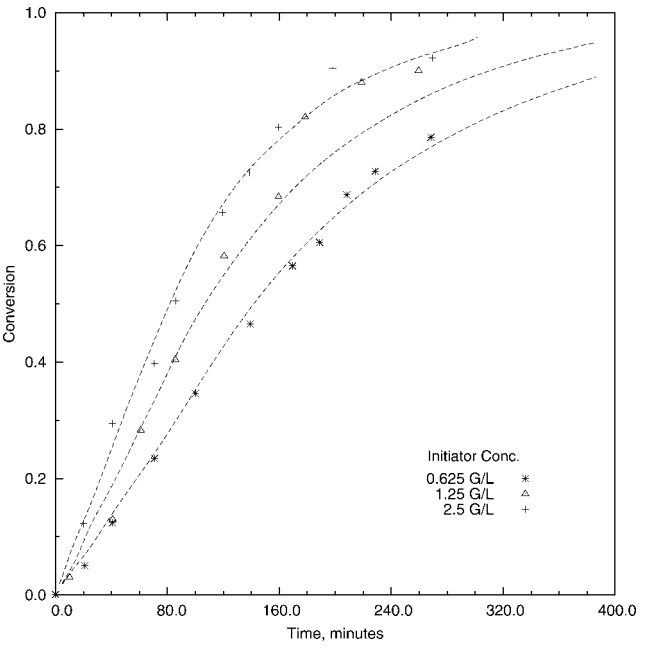

Figure 3 Comparison of the model prediction and experimental data[75] for the effect of [I] on the conversion–time behavior ([E] = 6.25 g/L, [M] = 0.5 g/cc).

The model predictions closely matched the experimental observations. For different emulsifier levels, the variation of Φ with X was the same. Φ inside the particles remained constant at the saturated Φ of 0.6 until X was equal to 0.41, and then, it started decreasing with X as $1 - X$. The close agreement between the experimentally reported variation of Φ with X and the model predictions seemed to justify the assumption that the effects of γ and particle size on Φ could be neglected.

Harada et al.[75] also reported the effects of [E], [I], and [M] on the progress of polymerization through conversion–time curves. As shown in Figures 2–4, good quantitative agreement was obtained between

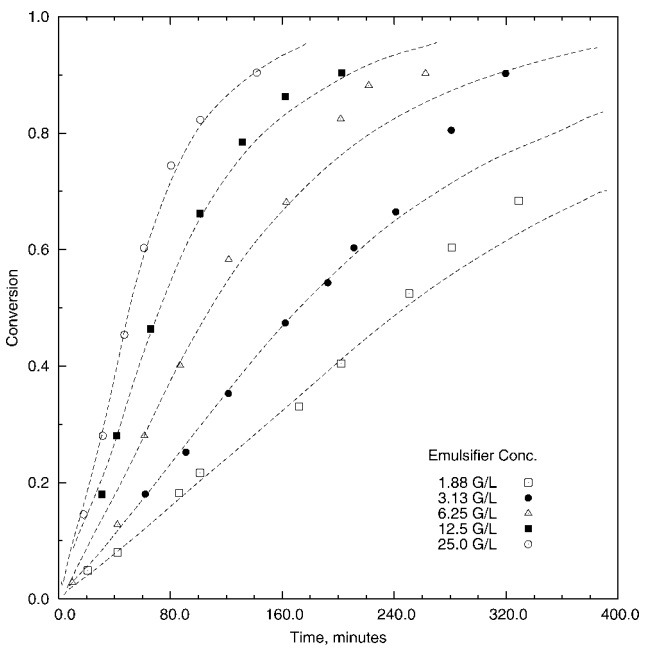

Figure 2 Comparison of the model prediction and experimental data[75] for the effect of [E] on the conversion–time behavior ([I] = 1.25 g/L, [M] = 0.5 g/cc).

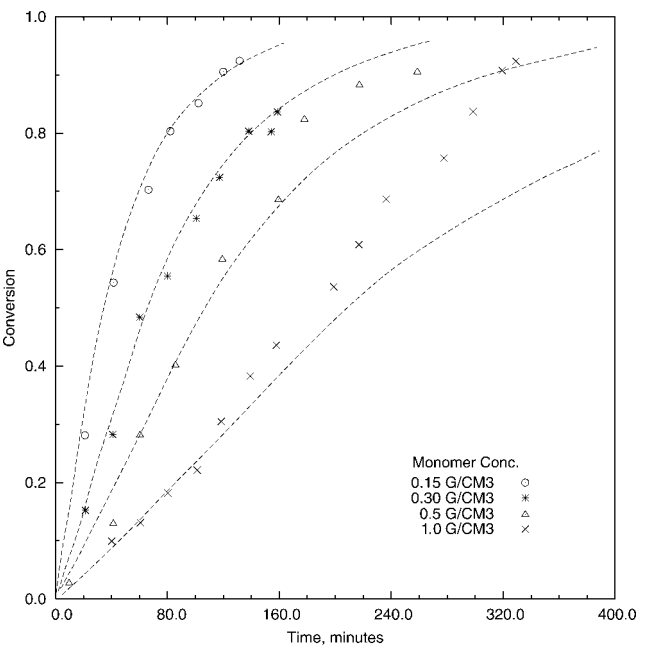

Figure 4 Comparison of the model prediction and experimental data[75] for the effect of [M] on the conversion–time behavior ([I] = 1.25 g/L, [E] = 6.25 g/L).

the model predictions (dotted lines) and the experimentally reported values (various markers), except in a few cases where the gel effect occurred.

In this work, I found ε to be 0.08. Furthermore, ε was found to be independent of [E], [I], and [M] and did not vary during the course of polymerization. In our previous study, in which we modeled the PSD for miniemulsion polymerization,[64] ε was found to be 0.009. Furthermore, ε was found to be independent of [I] and did not vary during the course of polymerization. Thus, the entry coefficients for radical capture by micelles and by miniemulsion droplets were much lower than those for the particles. The only difference between the micelles or droplets and the particles was that the particles were polymerizing, whereas the micelles and droplets were not. These differences were explained in terms of diffusion without reaction in case of the micelles and the droplets and diffusion with reaction in the case of the particles by Hansen–Ugelstad–Fitch–Tsai theory.[39] An alternate concept of activation energy as a barrier to radical entry was used in my recent article.[48] This approach has experimental support also; the first-order entry rate coefficient (ρ_I; expressed as the number of radicals entering per particle per second per unit reaction volume) was shown[97,98] to follow the Arrhenius law, that is, $\rho_I = \rho_o \exp(-E/R_G T)$, where ρ_o is the frequency factor and E is the activation energy. This concept was also used in the work of Jwranicova and Capek.[98] The differences in radical entry rates in micelles and miniemulsion droplets as compared to the particles could be explained in terms of a higher activation energy for radical entry into nonpolymerizing entities such as micelles or miniemulsion droplets compared to polymerizing entities such as particles.

CONCLUSIONS

The aim of this study was to develop and validate a mathematical model to predict the evolution of the latex PSD in an emulsion polymerization reactor. The mathematical model was formulated around the population balance approach. The two important phenomena, particle nucleation and particle growth, that are the major determinants of the latex PSD were modeled in detail. At this level, the model is applicable to situations when the initial emulsifier level is above cmc when coalescence is absent and micellar nucleation is the dominant nucleation mechanism.

The model predictions were in close quantitative agreement with the experimental data for the emulsion polymerization of styrene as taken from the literature. The model's reliability was demonstrated by successful simulation of the experimental data for a number of variables. The model predictions were compared to experimental measurements of N_P, t_n, X_n, the variation of Φ with X, and the conversion–time curves obtained for different [I], [E], and [M] values.

The close quantitative match between the model predictions and the experimental data could be largely attributed to the choice of values of the important parameters as calculated experimentally. There are no adjustable parameters in the model.

NOMENCLATURE

Symbols

a	parameter that accounts for the relative importance of radical entry with respect to radical termination
a_{em}	emulsifier coverage area on a micelle (cm^2/molecule)
a_{ep}	emulsifier coverage area on a particle (cm^2/molecule)
A_P	total particle surface area (cm^2)
b	parameter that accounts for the relative importance of radical exit with respect to radical termination inside the particle
dv	differential volume
D	particle diameter
D_m	effective diffusivity of the radical
E	activation energy (cal g/mol)
[E]	emulsifier concentration (g mol/cm^3)
$[E]_{cmc}$	critical micelle concentration (g/cm^3)
$[E]_f$	emulsifier concentration in the feed (g mol/cm^3)
$[E]_R$	emulsifier concentration in the reactor (g mol/cm^3)
$[E]_W$	free emulsifier in the aqueous phase
f	initiator efficiency
$F(v,t)V_R$ dv	number of particles with sizes between v and v + dv
$F(t',t)V_R$ dt′	number of particles with t′ between t′ and t′ + dt′
$F_i(v,t)dv$	number of particles having i radicals with sizes between v and $vtdv$
i, i_{avg}	average number of radicals per particle
$I_b(a)$	modified Bessel function of the first kind of order b and argument a
[I]	initiator concentration in the reactor (g mol/cm^3)
$[I]_f$	initiator concentration in the feed (g mol/cm^3)
k_d	initiator decomposition rate constant (s^{-1})
k_{de}	radical exit rate coefficient (s^{-1})
k_e	radical entry rate coefficient (s^{-1})
k_{mm}	entry coefficient for radical capture by micelles (cm^2/s)

k_{mp} entry coefficient for radical capture by particles (cm^2/s)
k_p propagation rate constant (cm^3 g mol^{-1} s^{-1})
k_t termination rate constant in the particle (cm^3 g mol/s)
k_{trm} coefficient of chain transfer to the monomer
k_{tw} termination rate constant in the aqueous phase (cm^3 g mol^{-1} s^{-1})
m_p mass of the polymer in the particle (g)
MW_E molecular weight of the emulsifier
MW_M molecular weight of the monomer
[m] micelle concentration in the reactor (g mol/cm^3)
[M] monomer concentration (g mol/cm^3)
$[M]_D$ monomer concentration in the droplet phase (g mol/cm^3)
$[M]_f$ monomer concentration in the feed (g mol/cm^3)
$[M]_P$ monomer concentration in the particle phase (g mol/cm^3)
$[M]_R$ monomer concentration in the reactor (g mol/cm^3)
$[M]_{sat}$ monomer concentration at saturation in the aqueous phase (g mol/cm^3)
$[M]_W$ monomer concentration in the aqueous phase (g mol/cm^3)
n exponent that determines whether radical capture is propagation-, diffusion-, or collision-controlled
N_a Avogadro's number
N_P total number of particles formed
[P] polymer concentration (g mol/cm^3)
$[P]_R$ polymer concentration in the reactor (g mol/cm^3)
Q_E volumetric flow rate of the emulsifier (cm^3/s)
Q_I volumetric flow rate of the initiator (cm^3/s)
Q_M volumetric flow rate of the monomer (cm^3/s)
r radius of the particle (cm)
R_{em} rate of radical capture by micelles (s^{-1})
R_{ep} rate of radical capture by particles (s^{-1})
R_g rate of particle mass growth (g/s)
R_G universal gas constant (cal g mol^{-1} K^{-1})
r_m radius of the micelle (cm)
R_n rate of micellar nucleation (g mol/s)
R_p rate of polymerization (g mol/s)
[R] aqueous phase radical concentration (g mol cm^3)
t time (s)
T absolute temperature (K)
t' birth time (s)
t_n duration of the nucleation period
v volume of the particle (cm^3)
V_D volume of the monomer droplets (cm^3)
V_M volume of the micelle (cm^3)
V_P volume of the polymer (cm^3)
V_R volume of the reaction mixture (cm^3)
V_W volume of the aqueous phase (cm^3)
X conversion
X_n conversion at the end of the nucleation period

Greek letters

γ interfacial tension (dyne/cm)
ε ratio of the entry coefficient of the radical entry into micelles to that into particles (k_{mm}/k_{mp})
Φ monomer volume fraction in the particle
Φ_{sat} equilibrium monomer volume fraction
ρ_I first-order entry rate coefficient (s^{-1})
ρ_M density of the monomer (g/cm^3)
ρ_o frequency factor (s^{-1})
ρ_P density of the polymer (g/cm^3)
χ Flory–Huggins interaction parameter

References

1. Yano, T.; Endo, K.; Nagamitsu, M.; Ando, Y.; Takigawa, T.; Ohmura, N. J Chem Eng Jpn 2007, 40, 228.
2. Vale, M. M.; McKenna, T. F. IEC Res 2007, 46, 643.
3. Park, M. J.; Dokuen, M. T.; Doyle, F. J., III. Macromol Theory Simul 2005, 14, 474.
4. Fortuny, M.; Graillat, C.; McKenna, T. F.; Araujo, P. H. H.; Pinto, J. C. AIChE J 2005, 51, 2521.
5. Do Amaral, M.; Van Es, S.; Asua, J. M. J Appl Polym Sci 2005, 47, 733.
6. Doyle, F. J., III; Harrison, C. A.; Crowley, T. J Comp Chem Eng 2003, 27, 1153.
7. Immanuel, C. D.; Doyle, F. J., III. Chem Eng Sci 2003, 58, 3681.
8. Zeaiter, J.; Romagnoli, J. A.; Barton, G. W.; Gomes, V. G.; Hawkett, B. S.; Gilbert, R. G. Chem Eng Sci 2002, 57, 2955.
9. Herrera-Ordonez, J.; Olayo, R. J Polym Sci Part A: Polym Chem 2000, 38, 2201.
10. Herrera-Ordonez, J.; Olayo, R. J Polym Sci Part A: Polym Chem 2000, 38, 2219.
11. Coen, E. M.; Gilbert, R. G.; Morrison, B. R.; Leube, H.; Peach, S. Polymer 1998, 39, 7099.
12. Mayer, M. J. J.; Meuldijk, J.; Thoenes, D. J Appl Polym Sci 1996, 59, 83.
13. Rawlings, J. B.; Ray, W. H. Polym Eng Sci 1988, 28, 237.
14. Rawlings, J. B.; Ray, W. H. Polym Eng Sci 1988, 28, 257.
15. Penlidis, A.; MacGregor, J. F.; Hamielec, A. E. J Coating Technol 1986, 58, 49.
16. Dougherty, E. P. J Appl Polym Sci 1986, 32, 3051.
17. Dougherty, E. P. J Appl Polym Sci 1986, 32, 3079.
18. Min, K. W.; Gostin, H. I. IEC Res 1979, 18, 272.
19. Min, K. W.; Ray, W. H. J Appl Polym Sci 1978, 22, 89.
20. Min, K. W.; Ray, W. H. J Macromol Sci Polym Rev 1974, 11, 177.
21. Sood, A. J Appl Polym Sci 2008, to appear.
22. Sood, A. Indian Chem Eng 2002, 44, 75.
23. Sood, A. J Appl Polym Sci 2004, 92, 2884.

24. Coen, E. M.; Peach, S.; Morrison, B. R.; Gilbert, R. G. Polymer 2004, 45, 3595.
25. Vale, H. M.; McKenna, T. F. Prog Polym Sci (Oxford) 2005, 30, 1019.
26. Saidel, G. M.; Katz, S. J Polym Sci Part C: Polym Symp 1969, 27, 149.
27. O'Toole, J. T. J Polym Sci Part C: Polym Symp 1969, 27, 171.
28. Rawlings, J. B. Ph.D. Thesis, University of Wisconsin, 1985.
29. Gao, J.; Penlidis, A. Prog Polym Sci 2002, 27, 403.
30. Chern, C. S. Prog Polym Sci (Oxford) 2006, 31, 443.
31. Herrera-Ordonez, J.; Olayo, R.; Carro, S. J Macromol Sci Polym Rev 2004, 44, 207.
32. Fitch, R. M. In Proceedings of the Water-Borne and Higher-Solids Coatings Symposium; University of Southern Mississippi, Hattiesburg, Mississippi, 2, 1981; p 25.
33. Emulsion Copolymerization and Particle Morphology: Future Directions in Polymer Colloids; El-Aasser, M. S.; Fitch, R. M., Eds.; Martinus Nijhoff: Boston, 1987.
34. Tauer, K.; Schellenberg, C.; Zimmermann, A. Macromol Symp 2000, 150, 1.
35. Hansen, F. K.; Ugelstad, J. J Polym Sci Polym Chem Ed 1978, 16, 1953.
36. Hansen, F. K.; Ugelstad, J. J Polym Sci Part A-1: Polym Chem 1979, 17, 3033.
37. Hansen, F. K.; Ugelstad, J. J Polym Sci Part A-1: Polym Chem 1979, 17, 3047.
38. Hansen, F. K.; Ugelstad, J. J Polym Sci Part A-1: Polym Chem 1979, 17, 3069.
39. Hansen, F. K.; Ugelstad, J. In Emulsion Polymerization; Piirma, I., Ed.; Academic: New York, 1982.
40. Harkins, W. D. J Chem Phys 1945, 13, 381.
41. Harkins, W. D. J Chem Phys 1946, 14, 47.
42. Smith, W. V.; Ewart, R. H. J Chem Phys 1948, 16, 592.
43. Priest, W. J. J Phys Chem 1952, 56, 1077.
44. Jacobi, B. Angew Chem 1952, 64, 539.
45. Fitch, R. M.; Tsai, C. H. In Polymer Colloids; Fitch, R. M., Ed.; Plenum: New York, 1971; p 73.
46. Roe, C. P. Ind Eng Chem 1968, 60, 20.
47. Maxwell, I. A.; Morrison, B. R.; Napper, D. H.; Gilbert, R. G. Macromolecules 1991, 24, 1629.
48. Sood, A. J Appl Polym Sci, to be submitted.
49. Prindle, J. C. Ph.D. Thesis, University of Wisconsin, 1989.
50. Tauer, K.; Kuhn, I Macromolecules 1995, 28, 2236.
51. Tauer, K.; Oz, N. Macromolecules 2004, 37, 5880.
52. Lichti, G.; Gilbert, R. G.; Napper, D. H. J Polym Sci Polym Chem Ed 1983, 21, 269.
53. Feeney, P. J.; Napper, D. H.; Gilbert, R. G. Macromolecules 1984, 17, 2520.
54. Morrison, B. R.; Maxwell, I. A.; Gilbert, R. G.; Napper, D. H. In Polymer Latexes; Daniels, E. S.; Sudol, E. D.; El-Aasser, M. S., Eds.; ACS Symposium Series 492; American Chemical Society: Washington, DC, 1992; p 28.
55. Morton, M.; Kaizerman, S.; Altier, M W J Colloid Sci 1954, 9, 300.
56. Hansen, F. K. In Polymer Latexes; Daniels, E. S.; Sudol, E. D.; El-Aasser, M. S., Eds.; ACS Symposium Series 492; American Chemical Society: Washington, DC, 1992; p 12.
57. Giannetti, E. AIChE J 1993, 39, 1210.
58. Abusleme, J. A.; Giannetti, E. Macromolecules 1991, 15, 4281.
59. Dunn, A. S. Proc ACS Div Polym Mater Sci Eng 1991, 64, 221.
60. Dunn, A. S. In Polymer Latexes; Daniels, E. S.; Sudol, E. D.; El-Aasser, M. S., Eds.; ACS Symposium Series 492; American Chemical Society: Washington, DC, 1992.
61. Carro, S.; Herrera-Ordonez, J. Macromol Rapid Commun 2006, 27, 274.
62. Ugelstad, J.; El-Aasser, M. S.; Vanderhoff, J. J Polym Sci Polym Lett Ed 1973, 3, 503.
63. Sood, A.; Awasthi, S. K. Macromol Theory Simul 2004, 13, 603.
64. Sood, A.; Awasthi, S. K. Macromol Theory Simul 2004, 13, 615.
65. Sood, A.; Awasthi, S. K. J Appl Polym Sci 2003, 88, 3058.
66. Asua, J. M. Prog Polym Sci (Oxford) 2002, 27, 1283.
67. Antonietti, M.; Landfester, K. Prog Polym Sci (Oxford) 2002, 27, 689.
68. El-Aasser, M. S.; Sudol, E. D. J Coat Tech Res 2004, 1, 20.
69. Schork, F. J.; Luo, Y.; Smulders, W.; Russum, J. P.; Butte, A.; Fontenot, K. Adv Polym Sci 2005, 175, 129.
70. Song, Z.; Poehlein, G. W. J Macromol Sci Chem 1988, 25, 403.
71. Shastry, V.; Garcia-Rubio, L. H. J Appl Polym Sci 2006, 100, 2847.
72. Shastry, V.; Garcia-Rubio, L. H. J Appl Polym Sci 2006, 100, 2858.
73. Schlueter, H. Macromolecules 1990, 23, 1618.
74. Varela de la Rosa, L.; Sudol, E. D.; El-Aasser, M. S.; Klein, A. J Polym Sci Part A: Polym Chem 1996, 34, 461.
75. Harada, M.; Nomura, M.; Kojima, H.; Eguchi, W.; Nagata, S. J Appl Polym Sci 1972, 16, 811.
76. Brooks, B. W. Br Polym J 1970, 2, 197.
77. Brooks, B. W. Br Polym J 1971, 3, 269.
78. Stockmayer, W. H. J Polym Sci 1957, 24, 314.
79. O'Toole, J. T. J Appl Polym Sci 1965, 9, 1291.
80. Ugelstad, J.; Mork, P. C.; Aasen, J. O. J Polym Sci Part A-1: Polym Chem 1967, 5, 2281.
81. Polymer Handbook, 3rd ed.; Brandrup, J.; Immergut, E. H., Eds.; Wiley-Interscience: New York, 1989.
82. Vijayendran, B. R. J Colloid Interface Sci 1977, 60, 418.
83. Gilbert, R. G.; Napper, D. H. Rev Macromol Rev Phys 1983, 23, 127.
84. Olive, C. H.; Olive, S. Makromol Chem 1960, 37, 71.
85. Koltoff, I. M.; Miller, I. K. J Am Chem Soc 1951, 73, 3055.
86. Fleischer, D. In Polymer Handbook, 3rd ed.; Brandrup, J.; Immergut, E. H., Eds.; Wiley-Interscience: New York, 1989.
87. Rudd, J. F. In Polymer Handbook, 3rd ed.; Brandrup, J.; Immergut, E. H., Eds.; Wiley-Interscience: New York, 1989.
88. Gardon, J. L. J Polym Sci Part A-1: Polym Chem 1968, 6, 2859.
89. CRC Handbook of Chemistry and Physics, 62nd ed.; Weast, R. C., Ed.; CRC: Boca Raton, FL, 1981.
90. Mead, R. N.; Poehlein, G. W. J Appl Polym Sci 1989, 38, 105.
91. Dunn, A. S. Br Polym J 1989, 25, 691.
92. Brooks, B. W. Br Polym J 1989, 21, 339.
93. Vanderhoff, J. W. J Polym Sci Polym Symp 1985, 72, 161.
94. Sood, A. M. S. Report, Lehigh University, 1991.
95. Schork, F. J.; Ray, W. H. J Appl Polym Sci 1983, 28, 407.
96. Nomura, M. In Emulsion Polymerization; Piirma, I., Ed.; Academic: New York, 1982.
97. Adams, M. E.; Trau, M.; Gilbert, R. G.; Napper, D. H.; Sangster, D. F. Aust J Chem 1988, 41, 799.
98. Fang, S.; Wang, K.; Pan, Z. Polymer 2003, 44, 1385.
99. Jwranicova, V.; Capek, I. Macromol Symp 2002, 179, 275.